University of Nebraska - Lincoln
DigitalCommons@University of Nebraska - Lincoln

Christian Binek Publications | Research Papers in Physics and Astronomy

Summer 6-20-2010

Robust isothermal electric control of exchange bias at room temperature

Xi He
University of Nebraska-Lincoln, lodgehixi@hotmail.com

Yi Wang
University of Nebraska-Lincoln, ywang1983@hotmail.com

Christian Binek
University of Nebraska-Lincoln, cbinek@unl.edu

Peter A. Dowben
University of Nebraska-Lincoln, pdowben@unl.edu

Follow this and additional works at: http://digitalcommons.unl.edu/physicsbinek

 Part of the Condensed Matter Physics Commons

He, Xi; Wang, Yi; Binek, Christian; and Dowben, Peter A., "Robust isothermal electric control of exchange bias at room temperature" (2010). *Christian Binek Publications*. 68.
http://digitalcommons.unl.edu/physicsbinek/68

This Article is brought to you for free and open access by the Research Papers in Physics and Astronomy at DigitalCommons@University of Nebraska - Lincoln. It has been accepted for inclusion in Christian Binek Publications by an authorized administrator of DigitalCommons@University of Nebraska - Lincoln.

nature materials

ARTICLES

PUBLISHED ONLINE: 20 JUNE 2010 | DOI: 10.1038/NMAT2785

Robust isothermal electric control of exchange bias at room temperature

Xi He[1], Yi Wang[1], Ning Wu[1], Anthony N. Caruso[2], Elio Vescovo[3], Kirill D. Belashchenko[1], Peter A. Dowben[1] and Christian Binek[1]*

Voltage-controlled spin electronics is crucial for continued progress in information technology. It aims at reduced power consumption, increased integration density and enhanced functionality where non-volatile memory is combined with high-speed logical processing. Promising spintronic device concepts use the electric control of interface and surface magnetization. From the combination of magnetometry, spin-polarized photoemission spectroscopy, symmetry arguments and first-principles calculations, we show that the (0001) surface of magnetoelectric Cr_2O_3 has a roughness-insensitive, electrically switchable magnetization. Using a ferromagnetic Pd/Co multilayer deposited on the (0001) surface of a Cr_2O_3 single crystal, we achieve reversible, room-temperature isothermal switching of the exchange-bias field between positive and negative values by reversing the electric field while maintaining a permanent magnetic field. This effect reflects the switching of the bulk antiferromagnetic domain state and the interface magnetization coupled to it. The switchable exchange bias sets in exactly at the bulk Néel temperature.

Spintronics strives to exploit the spin degree of freedom of electrons for an advanced generation of electronic devices[1,2]. In particular, voltage-controlled spin electronics is of vital importance to continue progress in information technology. The main objective of such an advanced technology is to reduce power consumption while enhancing processing speed, integration density and functionality in comparison with present-day complementary metal–oxide–semiconductor electronics[3–6]. Almost all existing and prototypical solid-state spintronic devices rely on tailored interface magnetism, enabling spin-selective transmission or scattering of electrons. Controlling magnetism at thin-film interfaces, preferably by purely electrical means, is a key challenge to better spintronics[7–10].

The absence of direct coupling between magnetization and electric field makes the electric control of collective magnetism in general, and surface and interface magnetism in particular, a scientific challenge. The significance of controlled interface magnetism started with the exchange-bias effect. Exchange bias is a coupling phenomenon at magnetic interfaces that manifests itself most prominently in the shift of the ferromagnetic hysteresis loop along the magnetic-field axis and is quantified by the magnitude $\mu_0 H_{EB}$ of the shift[11]. The exchange-bias pinning of ferromagnetic thin films is employed in giant magnetoresistance and tunnelling magnetoresistance structures of magnetic-field sensors and modern magnetic read heads[12].

Electric control of exchange bias has been proposed for various spintronic applications that go beyond giant magnetoresistance and tunnelling magnetoresistance technology[5]. One approach to such voltage control requires a reversible, laterally uniform, isothermal electric tuning of the exchange-bias field at room temperature, which remains a significant challenge.

Early attempts in electrically controlled exchange bias tried to exploit the linear magnetoelectric susceptibility of the antiferromagnetic material Cr_2O_3 as an active exchange-bias pinning system[13]. In a magnetoelectric material an applied electric field induces a net magnetic moment, which can be used to electrically manipulate the magnetic states of an adjacent exchange-coupled ferromagnetic film[14]. The small value of the maximum parallel magnetoelectric susceptibility $\alpha_{me}^{\parallel}(T = 263\,\mathrm{K}) \approx 4.13\,\mathrm{ps\,m^{-1}}$ of Cr_2O_3 (ref. 15) led many researchers to the conclusion that multiferroic materials are better suited for this purpose. Such materials have two or more ferroic order parameters, such as ferroelectric polarization and (anti)ferromagnetic order[16].

The potential for an increased magnetoelectric response, for the multiferroic materials, was dictated by the maximum possible value of α_{me}^{ij}. It is determined by the geometric mean of the ferroic susceptibilities, both of which can individually be very high in multiferroics[17–20]. Coupling between these order parameters has been demonstrated[21]. However, it is typically weak, and the theoretical upper limit of α_{me}^{ij} is rarely reached[16].

Artificial two-phase multiferroics have been studied extensively. Such piezoelectric/ferromagnetic heterosystems allow for electric control of anisotropy[22,23]. However, strain-induced non-hysteretic magnetoelastic effects are often not stable (persistent) in the absence of an applied field (that is, volatile). Removing the electric field from a linear piezoelectric element releases the strain in the ferromagnetic component and hence restores the anisotropy of the piezoelectrically unstrained film. When using a ferroelectric material, to induce piezoelectric strain control, one may take advantage of the ferroelectric hysteresis to impose some residual strain that will persist after removing the electric field. In contrast to this electric control of magnetic anisotropy in two-phase multiferroics, we report on a non-volatile electric control of unidirectional magnetic anisotropy.

The most promising multiferroic single-phase materials used for electrically controlled exchange bias are $YMnO_3$ and $BiFeO_3$ (refs 24,25). Complete suppression of the exchange bias has been

[1]Department of Physics & Astronomy and the Nebraska Center for Materials and Nanoscience, University of Nebraska, Lincoln, Nebraska 68588-0111, USA, [2]Department of Physics, 257 Flarsheim Hall, University of Missouri, 5110 Rockhill Road, Kansas City, Kansas 64110, USA, [3]Brookhaven National Laboratory, National Synchrotron Light Source, Upton, New York 11973, USA. *e-mail: cbinek2@unl.edu.

achieved at 2 K in an $YMnO_3$/NiFe (permalloy) heterostructure. This effect, however, is irreversible. Moreover, the limitation of low temperatures makes $YMnO_3$ unsuitable for applications. The situation is better with $BiFeO_3$. In $BiFeO_3$/CoFe heterostructures, local magnetization reversal on a lateral length scale of up to 2 μm has been demonstrated[25,26]. However, global magnetization reversal, which could be revealed in macroscopic magnetic hysteresis, has not been achieved. Global, but not isothermal magnetoelectric switching has been achieved in the pioneering Cr_2O_3/CoPt heterostructure[13]. However, each sign reversal of the exchange-bias field required a new magnetoelectric annealing procedure, in which the pinning layer is cooled from $T > T_N$ to $T < T_N$ in the presence of both electric and magnetic fields. Isothermal electric control of exchange bias has been attempted by various groups, but with only marginal success[27,28]. The result was that reversible and global electrically controlled exchange bias carried out isothermally at room temperature remained elusive.

Here we reveal an unconventional ferromagnetism at the (0001) surface of the magnetoelectric antiferromagnet Cr_2O_3 and demonstrate its suitability for electrically controlled exchange bias and magnetization. New insights were achieved by combining first-principles calculations, general symmetry arguments, spin-resolved photoemission spectroscopy and magnetometry (see Supplementary Information) for the Cr_2O_3 (0001) surface and its interface in an exchange-bias heterostructure. We used a molecular beam epitaxy (MBE)-grown chromia thin film (see the Methods section) for the spin- and energy-resolved ultraviolet photoemission spectroscopy (UPS), whereas the isothermal electric control of exchange bias was done on a heterostructure involving an oriented chromia single crystal with (0001) surface. The choice of a high-quality single crystal for the exchange-bias system completely rules out sample heating induced by leakage currents because of the virtually perfect insulating properties of single-crystalline chromia. The UPS measurements have been carried out in zero electric field after magnetoelectric initialization of the antiferromagnetic domain state. The non-zero conductivity of thin films is a well-known experimental advantage used for the photoemission investigation of samples that otherwise are virtually perfectly insulating in the bulk. The finite conductivity of the thin film prevents charge accumulation, which could lead to misrepresented photoelectron energies.

On the basis of the understanding of the surface ferromagnetism of Cr_2O_3 (0001), a new concept of Cr_2O_3 (0001)-based exchange bias is implemented. As a result, a reversible, isothermal and global electric control of exchange bias is demonstrated at room temperature by reproducible electrically induced discrete shifts of the global magnetic hysteresis loop along the magnetic-field axis (see Supplementary Movie).

Magnetically uncompensated surfaces of antiferromagnetically ordered single crystals have been a subject of intense investigations, in particular in the framework of exchange bias[11]. The surface magnetization of an uncompensated antiferromagnetic surface with roughness usually averages out, so that only a small non-equilibrium statistical fluctuation remains for exchange coupling with the adjacent ferromagnet[29].

The surfaces of single-domain antiferromagnetic magnetoelectrics, such as the (0001) surface of the antiferromagnetically long-range ordered Cr_2O_3, are remarkable exceptions. The free energy of this system, with a boundary, depends on the polar vector **n** (external normal) as a macroscopic parameter. The existence of the magnetization at the boundary can be deduced from the reduction of the bulk magnetic point group by the presence of an invariant vector **n**. As both **n** and **E** are polar vectors, the boundary reduces the symmetry in a similar way to the electric field, **E**, in the bulk. An equilibrium magnetization must therefore exist at the surface of a magnetoelectric antiferromagnet, or at its interface with another material. This argument automatically includes equilibrium surface roughness; a more detailed analysis will be published elsewhere.

Both the bulk single crystal and the thin-film sample are confirmed to be (0001) oriented by X-ray diffraction. The surface topography of the bulk and the thin-film sample are mapped using atomic force microscopy (AFM). Figure 1 is organized in such a way that structural data of the bulk sample are shown in the upper panels of a and b. The corresponding data of the thin-film sample are shown in the lower panels of Fig. 1a,b. The (0001) orientation of the bulk surface is independently corroborated by the hexagonal reflection pattern obtained in low-energy electron diffraction. The prominent (0006) and (00012) X-ray peaks of the bulk sample are virtually identically reproduced in the thin film (compare peak positions in the upper and lower panels of Fig. 1a). The surface topography of the samples reveals a plateau with a root-mean-squared (r.m.s.) roughness of 0.88 nm for the surface of the bulk crystal (upper panel of Fig. 1b) and an even lower r.m.s. roughness of 0.19 nm (lower panel of Fig. 1b) for the thin-film sample measured along selected lines.

Figure 1c illustrates a configuration of the Cr_2O_3 (0001) surface. It is seen that the particular antiferromagnetic domain has an uncompensated surface magnetic monolayer with aligned moments on all surface Cr^{3+} ions, even if the surface is not atomically flat. Two features conspire to produce this property. First, the corundum lattice of Cr_2O_3 can be imagined as a layered arrangement of buckled Cr^{3+} ions sandwiched between the triangular layers of O^{2-} ions[30]. The electrostatically stable charge-neutral surface of this crystal is terminated by a semi-layer of Cr; this termination can be viewed as the cleavage of the crystal in the middle of the buckled Cr^{3+} layer[31]. Second, Cr ions, which are structurally similar with respect to the underlying O layer, have parallel spins. As a result, a single-domain antiferromagnetic state has all surface Cr spins pointing in the same direction. Note that although we have shown the surface Cr ions in bulk-like positions in Fig. 1, this assumption is immaterial for the existence of the surface magnetization, as follows from the general symmetry argument.

In single-crystalline Cr_2O_3, the antiferromagnetic order allows two degenerate 180° antiferromagnetic domains[14] (see Fig. 1 and Supplementary Fig. S1). These two domains have surface magnetizations of opposite sign. If the degeneracy of the two domain types is not lifted, the system develops a random multi-domain state with zero net surface magnetization when it is cooled below T_N. However, magnetoelectric annealing allows for preferential selection of one of these 180° domains by exploiting the free-energy gain $\Delta F = \alpha EH$ (ref. 14). As a result, even a rough Cr_2O_3 (0001) surface becomes spin-polarized when an antiferromagnetic single-domain state is established. Evidence of this roughness-insensitive surface magnetism is revealed by magnetometry (Supplementary Fig. S2 and Discussion) as well as spin-resolved UPS. Interpretation of the latter is supported by calculations of the site-resolved density of states (DOS) revealing a spin-polarized surface band above the valence-band maximum, in agreement with experimental findings. The UPS carried out on our MBE-grown Cr_2O_3 (0001) sample is sensitive to occupied surface electronic states.

Figure 2a shows the spin-polarized photoelectron intensity versus binding energy measured at 100 K. First, the MBE-grown Cr_2O_3 (0001) thin film has been cooled from $T > T_N$ in a small magnetic field of 30 mT alone, into a multidomain antiferromagnetic state. Spin-up and spin-down photoelectron intensities $I_{\uparrow,\downarrow}$ (red circles and blue squares) are virtually identical, indicating negligible net surface magnetization and polarization.

Furthermore, multiple measurements were undertaken for the single-antiferromagnetic-domain states, each with a fresh sample preparation. Subsequent sample preparations involve alternating

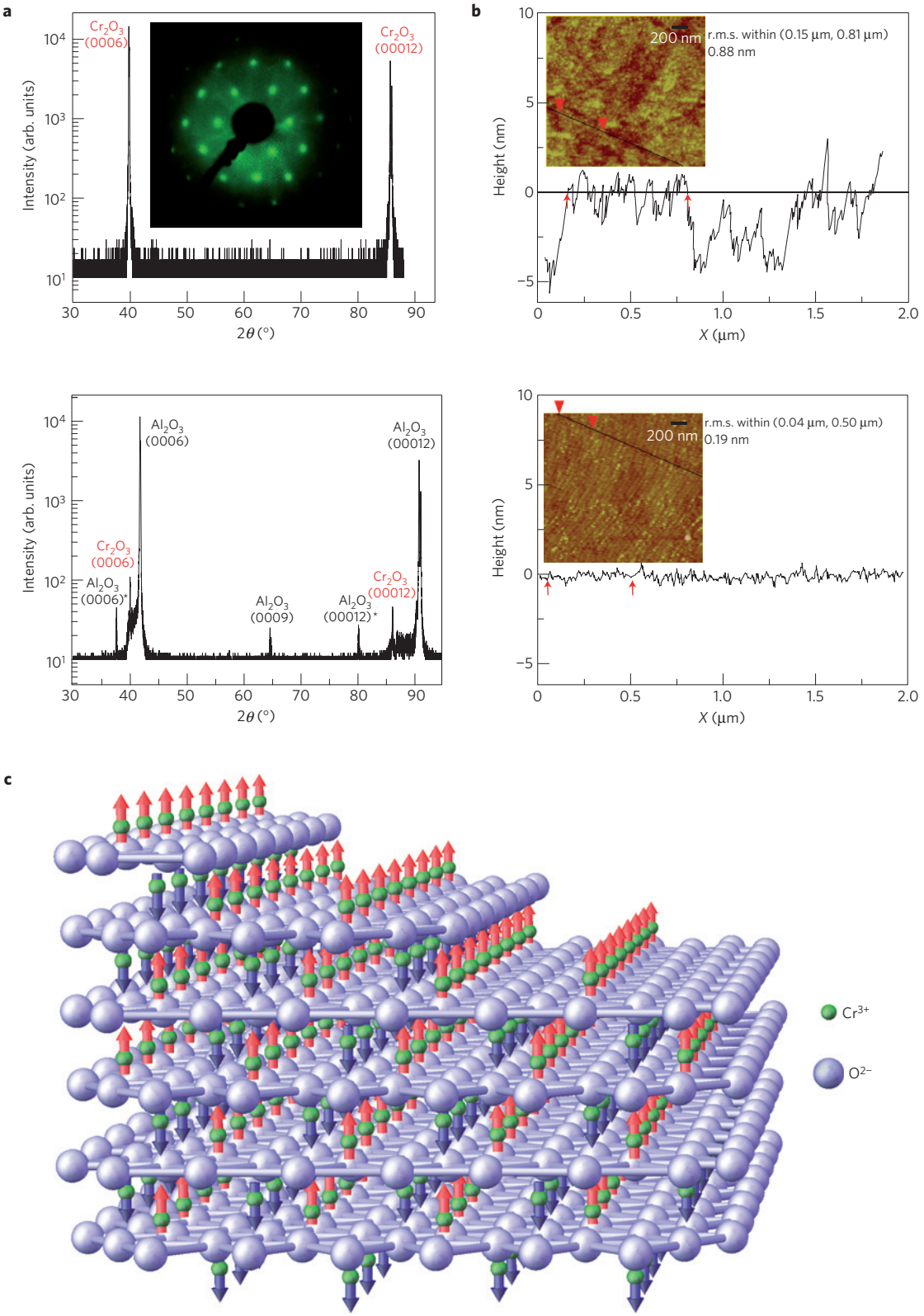

Figure 1 | Structural characterization. a, θ–2θ X-ray diffraction pattern of chromia bulk single crystal (upper panel) and thin film (lower panel) showing the chromia (0006) and (00012) peaks, respectively. The film is deposited on a sapphire (0001) substrate, giving rise to (0006), (00012), K_α and K_β (*) peaks and a weak structure-factor-forbidden (0009) peak. The inset shows a room-temperature low-energy electron diffraction pattern of the hexagonal chromia (0001) surface measured at an electron energy of 140 eV. **b**, Real-space topography of the chromia (0001) surface of bulk single crystal (upper panel) and thin film (lower panel) measured by AFM. The respective main frames show cross-sectional analysis along indicated lines. A r.m.s. roughness of 0.88 nm is calculated in the region between scanning position 0.15 and 0.81 μm for the bulk single crystal. The r.m.s. roughness of 0.19 nm of the thin film is measured between 0.04 and 0.50 μm. **c**, The spin structure of a Cr_2O_3 single crystal with a stepped (0001) surface is shown for one of its two antiferromagnetic single-domain states. Up (red) and down (dark blue) spins of the Cr^{3+} ions (green spheres) point along the *c* axis.

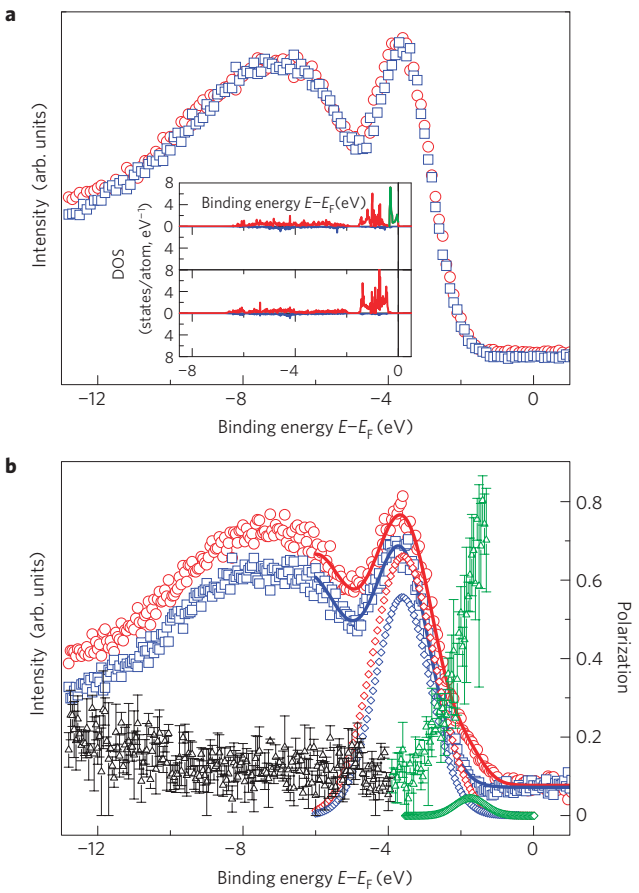

Figure 2 | Spin-polarized UPS measurements and layer-resolved DOS. **a**, The intensity of photoelectrons (occupied states) versus binding energy from a Cr_2O_3 (0001) surface measured at $T = 100$ K after cooling in $\mu_0 H = 30$ mT and $E = 0$ from $T > T_N$. Spin-up and spin-down intensities are shown by red circles and blues squares, respectively. Inset: The result of a first-principles calculation of the layer-resolved DOS. Colour code follows the experiment. The green line indicates a surplus surface state with spin-up polarization. **b**, Spin-up (red circles) and spin-down (blue squares) intensities after magnetoelectric annealing in $E = 3.85 \times 10^{-4}$ kV mm^{-1} and $\mu_0 H = 30$ mT. The lines are best fits of multiple-peak Gaussian functions. The diamonds show Cr 3*d* spin-up (red and green) and spin-down (blue) contributions extracted from the fits. The Gaussian fit shown by the green diamonds reflects specific surface states. Colour code matches the theoretical DOS data. The triangles show the contrast, *P*, in the spin-dependent intensities versus binding energy. The green triangles highlight the contribution from the surface state. Maximum absolute errors in *P* are indicated by bars.

magnetoelectric field cooling from above the Néel temperature to the target temperature of $T = 100$ K. The magnetoelectric annealing in alternating fields gives rise to alternating surface magnetization. This leads to a reproducible reversal of the spin-polarization measured at $T = 100$ K. Such data are then summed to provide an average overall net polarization, independent of instrumental asymmetry, as is the standard practice in spin-polarized photoemission and spin-polarized inverse photoemission.

The signal is clearly spin-split after magnetoelectric annealing in $E = 3.85 \times 10^{-4}$ kV mm^{-1} and $\mu_0 H = 30$ mT (compare red circles and blue squares in Fig. 2b), demonstrating high net spin-polarization at the surface. The spin contrast $P = (I_\uparrow - I_\downarrow)/(I_\uparrow + I_\downarrow)$, exhibited by triangles in Fig. 2b, is seen to increase significantly close to the valence-band maximum, E_F, (green triangles). We identify this feature with the contribution from the spin-polarized surface states of Cr 3*d* character. To corroborate this interpretation, we decompose the spin-dependent photoemission spectra $I_{\uparrow,\downarrow}$ into contributions from Cr 3*d* bulk and surface states. The contribution above the valence-band maximum (green) is interpreted as an extra spin-polarized surface state.

This interpretation is in accordance with our first-principles calculation of the layer-resolved DOS of the Cr_2O_3 (0001) surface shown in the inset of Fig. 2a. The DOS of a representative central layer with spin-up sublattice (majority/minority in red/blue) magnetization is shown by the lower two curves of the inset. The DOS of the surface layer is shown by the two upper curves in the inset of Fig. 2a. Note that in addition to the bulk states, a surplus spin-up density of states (green) appears above the valence-band maximum. This is consistent with our experimental findings in photoemission (Fig. 2b) and magnetometry (Supplementary Fig. S2 and Discussion).

Experimental and theoretical evidence together point very strongly to the existence of a roughness-insensitive ferromagnetic state at the Cr_2O_3 (0001) surface when the underlying Cr_2O_3 single crystal is in an antiferromagnetic single-domain state. Our findings indicate that the surface has a magnetization and is spin-polarized, despite the roughness that is evidently present according to our AFM investigations. Although the roughness may have some effect on the magnitude of the surface magnetization, its mere presence is unusual, and further supported by the experiments on electrically switched exchange bias.

The ferromagnetic surface moment can be isothermally switched by electrical means, giving rise to reversible switching of large exchange-bias fields in our perpendicular exchange-bias heterostructure Cr_2O_3(0001)/Pd 0.5 nm/(Co 0.6 nm Pd 1.0 nm)$_3$. The Cr_2O_3 substrate in the exchange-bias heterostructure is a (0001) bulk single crystal. The temperature dependence of the exchange bias and its relation to the temperature dependence of the chromia surface magnetization are discussed in the Supplementary Discussion.

Figure 3 demonstrates large isothermal electric switching of the exchange-bias field. It is achieved by leaving the realm of the linear magnetoelectric effect, which gives rise to only a minuscule electric control effect[27,28]. In contrast to this small linear effect, significant electrically controlled switching requires that a critical threshold given by the product $|EH|_c$, where E and H are isothermally applied axial electric and magnetic fields, is overcome. Initially the heterostructure has been magnetoelectrically annealed in $EH > 0$ with $E = 0.1$ kV mm^{-1} and $\mu_0 H = 77.8$ mT down to $T = 303$ K. The hysteresis loops are measured isothermally at $T = 303$ K and $E = 0$. The red squares in Fig. 3a,b show the same virgin loop with positive exchange bias of $\mu_0 H_{EB} = +6$ mT. Next, without changing the temperature, a field product $EH < 0$ of individual fields $E = -2.6$ kV mm^{-1} and $\mu_0 H = +154$ mT is applied for less than a second. During the time when an electric field is applied, the electric current is monitored to stay below 0.01 μA, resulting in virtually zero sample heating. After applying the electric- and magnetic-field product a magnetic hysteresis loop is measured in $E = 0$. Green triangles (Fig. 3a) show the resulting loop with a pronounced negative exchange bias of $\mu_0 H_{EB} \approx -13$ mT. The same field product is achieved with $E = +2.6$ kV mm^{-1} and $\mu_0 H = -154$ mT, having the same effect on the exchange bias as shown in Fig. 3b by blue circles. The isothermal switching of the exchange-bias field implies a field-induced switching of the antiferromagnetic single-domain state of Cr_2O_3 into the opposite antiferromagnetic registration. This switching is accompanied by a reversal of the interface magnetization. Figure 3c shows a sequence of switched exchange-bias fields obtained by switching the electric field back and forth between $E = +2.6$ kV mm^{-1} and $E = -2.0$ kV mm^{-1} at constant set field $\mu_0 H = -154$ mT, all at a constant temperature $T = 303$ K. The reproducible switching shows no signs of ageing. The asymmetry between positive and negative

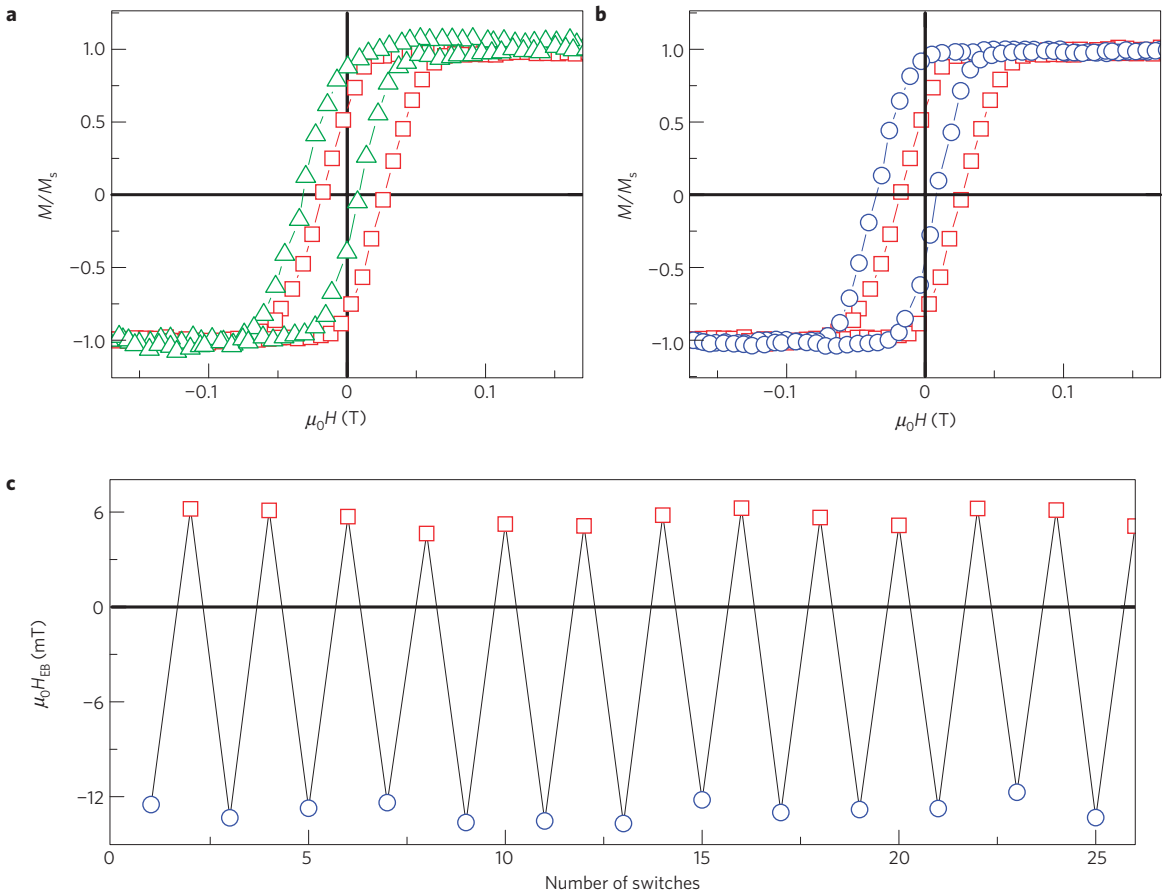

Figure 3 | Isothermal electric switching of the exchange-bias field. a, Exchange-biased hysteresis loops of Cr_2O_3 (0001)/Pd 0.5 nm/(Co 0.6 nm Pd 1.0 nm)$_3$ at $T = 303$ K after initial magnetoelectric annealing in $E = 0.1$ kV mm^{-1} and $\mu_0 H = 77.8$ mT. Hysteresis loops are measured by polar Kerr magnetometry in $E = 0$, respectively. The red squares show the virgin curve with a positive exchange-bias field of $\mu_0 H_{EB} = +6$ mT. Isothermal-field exposure in $E = -2.6$ kV mm^{-1} and $\mu_0 H = +154$ mT gives rise to a loop with a negative exchange-bias field of $\mu_0 H_{EB} \approx -13$ mT (green triangles). **b**, The red squares show the same virgin reference loop. The blue circles show the hysteresis loop after isothermal-field exposure in $E = +2.6$ kV mm^{-1} and $\mu_0 H = -154$ mT, giving rise to the same negative exchange bias of $\mu_0 H_{EB} = -13$ mT. **c**, $\mu_0 H_{EB}$ versus number of repeated isothermal switching through exposure to $E = +2.6$ kV mm^{-1} (blue circles) and $E = -2$ kV mm^{-1} (red squares) at constant $\mu_0 H = -154$ mT, respectively.

exchange-bias values is a consequence of a difference in the interface magnetization $S_{Cr_2O_3}$ for negative and positive exchange bias.

A nonlinear magnetoelectric switching of the antiferromagnetic single-domain state of Cr_2O_3 was reported as far back as 1966 by Martin and Anderson[32]. Their work illustrated that the isothermal switching between the two different antiferromagnetic domains of Cr_2O_3 is possible if sufficiently strong field products $E \cdot H$ are applied along the c axis[32]. This switching is a thermally activated process. At constant temperature there is a critical value $|EH|_c$, above which the system settles into the single-domain state with the lowest free energy, even if this requires a switching of the entire antiferromagnetic spin structure. This hysteretic switching of Cr_2O_3 is directly reflected in the hysteresis of the electric-field dependence of the exchange-bias field.

Figure 4 shows the threshold character of electric switching at $T = 303$ K. All data are taken after magnetoelectric annealing in $E = 0.1$ kV mm^{-1} and $\mu_0 H = 77.8$ mT. The hysteretic electric-field dependence, $\mu_0 H_{EB}$ versus E, is determined from individual magnetic hysteresis loops measured in $E = 0$. Each data point results from a loop measured after isothermal exposure of the sample to one of various E-fields and fixed magnetic field $\mu_0 H = -115$ mT (circles), $\mu_0 H = -154$ mT (triangles) and $\mu_0 H = -229$ mT (squares), respectively. Note that the same values of the field products can be achieved for various corresponding positive magnetic fields $\mu_0 H = +115, +154$ and $+229$ mT. The resulting electrically controlled switching is shown in Supplementary Fig. S4. Two main characteristics are observed in the $\mu_0 H_{EB}$ versus E data. First, for a given positive magnetic field there is a critical negative and positive electric field, E_c, where switching of the exchange-bias field takes place. The rectangular hysteresis $\mu_0 H_{EB}$ versus E is in perfect agreement with the isothermal switching of the antiferromagnetic domain state of Cr_2O_3 reported in ref. 32. This includes details such as the asymmetry between the negative and the positive switching field.

The insets of Fig. 4 show that the critical switching fields of the exchange bias obey the relation $|EH|_c = \text{const}$ corresponding to the switching of the Cr_2O_3 antiferromagnetic single domain[32]. Solid squares are data points of E_c for magnetic fields $\mu_0 H = -115, -154$ and -229 mT. The lines are fits of the functional form $H = \text{const}/E_c$. This shows that the switching effect originates from the coherent flip of the antiferromagnetic registration of the Cr_2O_3 pinning system. The inversion of the antiferromagnetic spin structure is accompanied by the reversal of the Cr_2O_3 (0001) interface magnetization, which in turn causes switching of the exchange-bias field. As this switching is induced at a threshold of the product $|EH|_c$, the H-field can be made arbitrarily small when E is scaled up accordingly. There is plenty of room for E-field increase by shrinking the thickness of the pinning layer down to the nanoscale. It is feasible to use nanostructured arrays of permanent magnetic nanopillars to apply magnetic stray

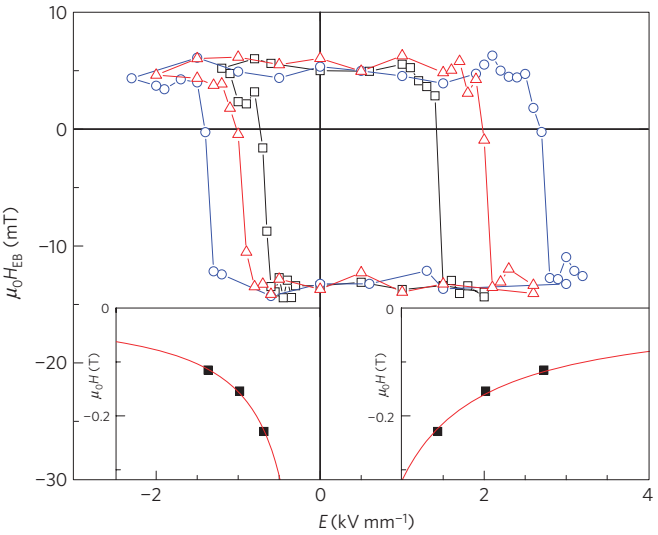

Figure 4 | Hysteretic electric-field dependence of the exchange-bias field. $\mu_0 H_{EB}$ versus E, measured at $T = 303$ K from individual Kerr loops. Data are taken after initial magnetoelectric annealing of Cr_2O_3 (0001)/Pd 0.5 nm/(Co 0.6 nm Pd 1.0 nm)$_3$ in axial fields $E = 0.1$ kV mm^{-1} and $\mu_0 H = 77.8$ mT. Kerr loops are measured in $E = 0$ after isothermal E-field and simultaneous H-field exposure of the sample. For a given $\mu_0 H_{EB}$ versus E curve the magnetic field is constant. The three $\mu_0 H_{EB}$ versus E data sets correspond to $\mu_0 H = -115$ mT (circles), $\mu_0 H = -154$ mT (triangles) and $\mu_0 H = -229$ mT (squares), respectively. The solid squares in the insets show the data points of electric switching fields and corresponding magnetic fields $\mu_0 H = -115, -154$ and -229 mT. The lines are single-parameter fits of the functional form $H = \text{const}/E_c$.

fields below the coercive field of the CoPd film. For instance, the field 20 nm from the end of a Ni rod, 175 nm long and 20 nm diameter, has been estimated as ~25 mT (ref. 33). The insets of Fig. 4 show that a magnetic stray field of 20 mT requires a maximum electric switching field of 16 kV mm^{-1} to reverse the exchange-bias field and ferromagnetic magnetization. Chromia is known for its excellent dielectric properties, and is used as a good insulator with high dielectric breakdown fields of 10^7 V cm^{-1} = 1,000 kV mm^{-1} at room temperature. Still it will remain a challenge to achieve these dielectric properties in thin films.

Electric control of magnetism, at room temperature, is the basis of advanced spintronics for post-metal–oxide–semiconductor technology. The intensive research efforts on multiferroic materials of recent years are to a large extent driven by the possibilities of electrically controlled magnetism at room temperature. We have shown by a combination of experiment and theory that Cr_2O_3, the archetypical magnetoelectric antiferromagnet, is revived as a candidate for reversible electric control of magnetism at room temperature. This control is made possible by the roughness-insensitive ferromagnetic spin state at the (0001) surface of Cr_2O_3. In the highly nonlinear magnetoelectric regime the antiferromagnetic order can be electrically switched along with the surface magnetization. This phenomenon takes place at the interface between Cr_2O_3 (0001) and a ferromagnetic Co/Pd multilayer film. In this perpendicular exchange-bias system, a reversible and global electric switching of the exchange-bias field was realized isothermally at room temperature. This observation opens up exciting prospects for spintronics applications.

Methods

MBE is used for the sample growth. *Ex situ* structural characterization is done by X-ray diffraction techniques. The magnetic characterization is primarily based on the polar magneto–optical Kerr effect and partially carried out with the help of a superconducting quantum interference device. The Cr_2O_3 (0001) surface of the c−Al_2O_3/Cr(110)[8 nm]/Cr_2O_3(0001)[103 nm] sample was cleaned by ion-beam sputtering and post-sputtering annealing procedures before the photoemission measurements. Spin-polarized angle-resolved photoemission spectra were acquired at the U5UA undulator spherical grating monochromator beamline at the National Synchrotron Light Source. The electronic structure calculations of the Cr_2O_3 (0001) surface were carried out using the projected augmented wave method as implemented in the Vienna *ab initio* simulation program[34–36].

Received 30 December 2009; accepted 18 May 2010; published online 20 June 2010

References

1. Wolf, S. A. *et al.* Spintronics: A spin-based electronics vision for the future. *Science* **294,** 1488–1495 (2001).
2. Žutić, I., Fabian, J. & Das Sarma, S. Spintronics: Fundamentals and applications. *Rev. Mod. Phys.* **76,** 323–410 (2004).
3. Zhirnov, V. V., Hutchby, J. A., Bourianoff, G. I. & Brewer, J. E. Emerging research logic devices. *IEEE Circuits Devices* **21,** 37–46 (2005).
4. Ney, A., Pampuch, C., Koch, R. & Ploog, K. H. Programmable computing with a single magnetoresistive element. *Nature* **425,** 485–487 (2003).
5. Binek, Ch. & Doudin, B. Magnetoelectronics with magnetoelectrics. *J. Phys. Condens. Matter* **17,** L39–L44 (2005).
6. Dery, H., Dalal, P., Cywiński, Ł. & Sham, L. J. Spin-based logic in semiconductors for reconfigurable large-scale circuits. *Nature* **447,** 573–576 (2007).
7. Zavaliche, F. *et al.* Electrically assisted magnetic recording in multiferroic nanostructures. *Nano Lett.* **7,** 1586–1590 (2007).
8. Tsymbal, E. Y. & Kohlstedt, H. Applied physics: Tunneling across a ferroelectric. *Science* **313,** 181–183 (2006).
9. Maruyama, T. *et al.* Large voltage-induced magnetic anisotropy change in a few atomic layers of iron. *Nature Nanotech.* **4,** 158–161 (2008).
10. Velev, J. P., Dowben, P. A., Tsymbal, E. Y., Jenkins, S. J. & Caruso, A. N. Interface effects in spin-polarized metal/insulator layered structures. *Surf. Sci. Rep.* **63,** 400–425 (2008).
11. Nogués, J. & Schuller, I. K. Exchange bias. *J. Magn. Magn. Mater.* **192,** 203–232 (1999).
12. Chappert, C., Fert, A. & Van Dau, F. N. The emergence of spin electronics in data storage. *Nature Mater.* **6,** 813–823 (2007).
13. Borisov, P., Hochstrat, A., Chen, X., Kleemann, W. & Binek, Ch. Magnetoelectric switching of exchange bias. *Phys. Rev. Lett.* **94,** 117203 (2005).
14. O'Dell, T. H. *The Electrodynamics of Magneto–Electric Media* (North-Holland, 1970).
15. Borisov, P., Hochstrat, A., Shvartsman, V. V. & Kleemann, W. Superconducting quantum interference device setup for magnetoelectric measurements. *Rev. Sci. Instrum.* **78,** 106105 (2007).
16. Fiebig, M. Revival of the magnetoelectric effect. *J. Phys. D* **38,** R123–R152 (2005).
17. Wang, J. *et al.* Epitaxial $BiFeO_3$ multiferroic thin film heterostructures. *Science* **299,** 1719–1722 (2003).
18. Hur, N. *et al.* Electric polarization reversal and memory in a multiferroic material induced by magnetic fields. *Nature* **429,** 392–395 (2004).
19. Eerenstein, W., Mathur, N. D. & Scott, J. F. Multiferroic and magnetoelectric materials. *Nature* **442,** 759–765 (2006).
20. Bibes, M. & Barthélémy, A. Multiferroics: Towards a magnetoelectric memory. *Nature Mater.* **7,** 425–426 (2008).
21. Lottermoser, T. *et al.* Magnetic phase control by an electric field. *Nature* **430,** 541–544 (2004).
22. Sahoo, S. *et al.* Ferroelectric control of magnetism in $BaTiO_3$/Fe heterostructures via interface strain coupling. *Phys. Rev. B* **76,** 092108 (2007).
23. Weiler, M. *et al.* Voltage controlled inversion of magnetic anisotropy in a ferromagnetic thin film at room temperature. *New J. Phys.* **11,** 013021 (2009).
24. Laukhin, V. *et al.* Electric-field control of exchange bias in multiferroic epitaxial heterostructures. *Phys. Rev. Lett.* **97,** 227201 (2006).
25. Chu, Y-H. *et al.* Electric-field control of local ferromagnetism using a magnetoelectric multiferroic. *Nature Mater.* **7,** 478–482 (2008).
26. Zhao, T. *et al.* Electrical control of antiferromagnetic domains in multiferroic $BiFeO_3$ films at room temperature. *Nature Mater.* **5,** 823–829 (2006).
27. Liu, J. P., Fullerton, E., Gutfleisch, O. & Sellmyer, D. J. (eds) in *Nanoscale Magnetic Materials and Applications* Ch. 6 (Springer, 2009).
28. Lim, S-H. *et al.* Exchange bias in thin-film $(Co/Pt)_3/Cr_2O_3$ multilayers. *J. Magn. Magn. Mater.* **321,** 1955–1958 (2009).
29. Kuch, W. *et al.* Tuning the magnetic coupling across ultrathin antiferromagnetic films by controlling atomic-scale roughness. *Nature Mater.* **5,** 128–133 (2006).
30. Krichevtsov, B. B., Pavlov, V. V. & Pisarev, R. V. Nonreciprocal optical effects in antiferromagnetic Cr_2O_3 subjected to electric and magnetic fields. *Zh. Eksp. Teor. Fiz.* **94,** 284–295 (1988).

31. Freund, H-J., Kuhlenbeck, H. & Staemmler, V. Oxide surfaces. *Rep. Prog. Phys.* **59,** 283–347 (1996).
32. Martin, T. J. & Anderson, J. C. Antiferromagnetic domain switching in Cr_2O_3. *IEEE Trans. Magn.* **2,** 446–449 (1966).
33. Bromwich, T. J. *et al.* Remanent magnetic states and interactions in nano-pillars. *Nanotechnology* **17,** 4367–4373 (2006).
34. Kresse, G. & Hafner, J. *Ab initio* molecular dynamics for open-shell transition metals. *Phys. Rev. B* **48,** 13115–13118 (1993).
35. Kresse, G. & Furthmueller, J. Efficiency of *ab inito* energy calculations for metals and semiconductors using a plane-wave basis set. *Comput. Mater. Sci.* **6,** 15–50 (1996).
36. Kresse, G. & Furthmueller, J. Efficient iterative schemes for *ab initio* total-energy calculations using a plane-wave basis set. *Phys. Rev. B* **54,** 11169–11186 (1996).

Acknowledgements

This work is supported by NSF through Career DMR-0547887, by the Nebraska Research Initiative (NRI), by the NSF MRSEC Grant No. 0820521 and by the NRC/NRI supplement to MRSEC. K.D.B. is a Cottrell Scholar of Research Corporation. Technical help from S-Q. Shi, V. R. Shah and L. P. Yue in the calculation of DOS, taking XRD and AFM data is acknowledged, respectively. We are thankful to Crystal GmbH for providing excellent Cr_2O_3 single crystals.

Author contributions

X.H. and C.B. designed the study, in particular conceiving the electrically controlled exchange bias and electrically controlled magnetism. Y.W. and X.H. collected and analysed the magnetic data. N.W. led the photoemission experiments and data analysis. A.C. and E.V. supported the photoemission experiments. K.D.B. conceived the concept of roughness-insensitive surface magnetization and directed the electronic structure calculations. P.A.D. directed and conceived the photoemission experiments. C.B. directed the overall study. All authors contributed to the scientific process and the refinement of the manuscript. C.B. and X.H. wrote most of the paper.

Additional information

The authors declare no competing financial interests. Supplementary information accompanies this paper on www.nature.com/naturematerials. Reprints and permissions information is available online at http://npg.nature.com/reprintsandpermissions. Correspondence and requests for materials should be addressed to C.B.